Eur. Phys. J. D **35**, 193–198 (2005)
DOI: 10.1140/epjd/e2005-00216-4

THE EUROPEAN PHYSICAL JOURNAL D

Nondissociative electron attachment to molecules and clusters

I.I. Fabrikant[a]

Department of Physics and Astronomy, University of Nebraska-Lincoln, Lincoln, NE 68588, USA

Received 5 April 2005
Published online 9 August 2005 –

Abstract. We present results of effective range theory calculations of nondissociative electron attachment to SF_6 molecules and CO_2 clusters. The first process is strongly influenced by the SF_6^- virtual state, and the second by vibrational Feshbach resonances associated with electron capture by the long-range polarization field of the cluster with simultaneous vibrational excitation of one molecular unit. We also study how both processes depend on the initial vibrational excitation of the target. We obtain a noticeable dependence of the attachment cross-section on the symmetric stretch vibration of SF_6, although it does not lead to a significant temperature dependence at low electron energies.

PACS. 34.80.Ht Dissociation and dissociative attachment by electron impact – 34.80.Gs Molecular excitation and ionization by electron impact – 36.40.Wa Charged clusters

1 Introduction

Electron collisions with molecules and clusters often involve electron capture which can be accompanied by a target fragmentation, a process called dissociative attachment [1]. However, in many cases, particularly for complex targets, attachment occurs without fragmentation, with formation of the parent ion. The well-known example involving a relatively simple target is low-energy electron attachment to SF_6 molecule. Others include electron attachment to van der Waals clusters [2] and molecules of biological interest [3].

The nondissociative electron attachment process is difficult for ab initio theoretical description. Indeed, nondissociative attachment occurs due to intramolecular vibrational energy redistribution (IVR) which involves many vibrational degrees of freedom. Specifically, due to interaction between initially excited vibrational mode (so-called specific mode) and numerous other modes (so-called bath modes) in the system, the initial excitation energy is becoming randomly redistributed among many vibrational degrees of freedom [4]. This process has been well studied in molecular spectroscopy [5] by applying classical dynamics and statistical models. However, it is much less studied in electron collisions since the first stage of the process, electron capture due to interaction with a specific vibrational mode, should be described quantum-mechanically. Thoss and Domcke [6] developed a quantal model including coupling between specific and bath modes. Due to difficulties of ab initio calculation of the coupling parameter, it was considered as a phenomenological one. More recently, using these ideas, we developed a theory of electron attachment to SF_6 molecules [7] and CO_2 clusters [8]. The case of CO_2 clusters is particularly interesting because it provides a theoretical description of vibrational Feshbach resonances (VFRs) [9–11] which occur due to electron capture in the long-range polarization potential of the cluster with a simultaneous vibrational excitation of one molecular unit.

The present paper reviews these developments and provides further information on electron scattering by CO_2 clusters including the analysis of VFRs in vibrational excitation and attachment from excited states.

2 Theoretical approach

We base our theoretical approach on a generalization of the multi-channel effective range theory (ERT) [4] which incorporates the electron attachment channel. To formulate this generalization, it is convenient to start from the R-matrix theory. We divide the whole space into two regions separated by a sphere of radius r_0. Outside the sphere we include only the long-range part of electron interaction with the target. In the case of the SF_6 molecule this is the isotropic polarization interaction plus geometry-dependent dipolar interaction responsible for excitation of the infrared-active ν_3 mode. In the case of a cluster the situation is more complicated since the size of a cluster is typically greater than r_0. If the electron is inside the cluster, we adopt the continuum medium approximation model [12] and represent the interaction V in the form

$$V = V_0 + \frac{a}{N^{1/3}}, \tag{1}$$

[a] e-mail: ifabrikant1@unl.edu

where V_0 is the excess electron energy in the bulk, N is the cluster size, i.e. number of molecular units in the cluster, and a is a positive constant related to the dielectric constant of the bulk medium and the Wigner-Seitz radius [12]. Our estimate [13] for the CO_2 clusters is $V_0 = -0.65$ eV, $a = 0.85$ eV. Outside the cluster we describe the interaction by the isotropic polarization potential $-\alpha_N/2r^4$, where $\alpha_N = N\alpha$, and α is the polarizability of one molecular unit. To make sure that this step-wise potential does not produce spurious effects in the cross-sections, we introduce a soft boundary between the two regions.

The wave function ψ, incorporating this interaction outside the R-matrix sphere, is matched with the internal wave function in the fixed-nuclei approximation in the form

$$\psi(r_0, q) = R(q)\frac{d\psi(r,q)}{dr}\bigg|_{r=r_0} \tag{2}$$

where r stands for the electron radial coordinate, and q for the set of all internuclear coordinates of the target. To obtain the R-matrix with the account of nuclear dynamics, we use the Born-Oppenheimer approximation [14]. First we write the fixed nuclei R-matrix in the form

$$R(q) = \sum_{\lambda=0}^{\infty} \frac{\gamma_\lambda^2(q)}{E_\lambda(q) - E_e} \tag{3}$$

where E_λ and γ_λ are eigenvalues and surface amplitudes for the fixed-nuclei problem, and E_e is the electron energy. We are mostly interested in s-wave scattering when the poles $E_\lambda(q)$ do not represent resonance states. However, the lowest pole ($\lambda = 0$) represents a bound state in the range of q where the negative ion is stable.

We will assume now that the q-dependence and the energy dependence of all terms in sum (3) except the first is weak so that $R(q)$ can be rewritten in the form

$$R(q) = \frac{\gamma_0^2(q)}{E_0(q) - E_e} + R_b, \tag{4}$$

where the background term R_b is independent of q and E_e. This is the usual assumption of the resonance R-matrix theory [15,16]. It is justified in our case as well because the interaction between the electron motion and the nuclear motion is weak in electronically excited states ($\lambda > 0$), and the electron energy E_e is small compared to the potential energy of interaction between the electron and the molecule.

We now include nuclear motion by adding the kinetic energy operator in the denominator of the R-matrix. As a result, R becomes an integral operator

$$R(q) = \gamma_0(q)(H_I - E)^{-1}\gamma_0(q) + R_b \tag{5}$$

where E is the total energy of the system, $H_I = T(q) + U(q)$, and $U(q) = E_0(q) + V(q)$, where T is the kinetic energy operator for the nuclear motion, $V(q)$ is the potential energy surface for the neutral molecule. In the presence of a dissociative attachment channel we modify the R operator by the replacement $E \to E + i0$. This corresponds to outgoing-wave boundary conditions when one of the internuclear coordinates goes to infinity. However, in the present paper we are interested in nondissociative attachment which occurs due to IVR whereby the vibrational energy initially concentrated in the active modes is redistributed among bath modes and is thus not available for autodetachment of the electron on the time scale of the experiment. In the case of the SF_6 molecule the active mode is the symmetric ν_1 ("breathing") vibrations [4], and in the case of electron attachment to CO_2 clusters there are two active modes: symmetric stretch and bending vibrations of one molecular unit.

A complete ab initio treatment of IVR requires calculations of the vibrational dynamics on the multidimensional potential surface $U(q)$. Thoss and Domcke [6] showed that the problem can be simplified in the Markov approximation for the interaction between the active mode and the bath modes by adding an energy independent width and shift to the system Hamiltonian, that is to the part of the Hamiltonian containing the coordinates of only the active mode. Accordingly we will replace the Hamiltonian $H_I(q)$ by $H_I^e(s) = T(s) + U(s) - i\Gamma(s)/2$, where s is the set of active vibrational coordinates. Like in the optical model, H and the R operator become now non-Hermitian, and the attachment cross-section is determined from the S-matrix unitarity defect.

The attachment dynamics is controlled by the energy region close to the pole of the operator $(H_I^e - E)^{-1}$. Therefore, to develop ERT, we rewrite equation (2) in the form

$$\frac{d\psi}{dr} = (R^e)^{-1}(s, E)\psi, \tag{6}$$

with

$$R^e(s, E) = \gamma_0(s)(H_I^e(s) - E)^{-1}\gamma_0(s) + R_b, \tag{7}$$

where all arguments of γ_0 other than s are taken at the equilibrium internuclear separation.

We will return now to the fixed-nuclei approximation at $r < r_0$ and replace the complex operator $(R^e)^{-1}(s, E)$ by a complex function $f(s, E)$. This approach is consistent with the frame transformation theory [17]: we assume that the time spent by electron in the inner region during the capture process is short compared to the vibrational period, and therefore the electron motion can be treated in the fixed-nuclei approximation. In contrast, the full vibrational dynamics should be incorporated in the outer region. This is done by solving vibrational close coupling equations at $r > r_0$.

In the spirit of the ERT of Gauyacq and Herzenberg [4,18], we expand $f(s, E)$ in powers of s (assuming that $s = 0$ corresponds to equilibrium) and keep only the lowest-order terms. In the case of the SF_6 molecule we assume only one active mode, and the expansion has the form

$$f = f_0 + f_1 s, \tag{8}$$

where f_0 and f_1 are complex parameters which generally depend on the electron energy. (Note, however, that the strongly infrared-active ν_3 mode *is* included in the external region.) In the first order approximation of ERT,

we neglect this energy dependence and consider f_0 and f_1 as complex constants. They are determined from the experimental data on attachment [19,20] and total [21] cross-sections at several energy points within the interval between 0.01 and 0.18 eV. In the case of CO_2 clusters we assume two active normal coordinates s and ρ, describing symmetric stretch and bending vibrations of one molecular units. In our calculations the ERT expansion of the function $f(s,\rho)$ contains four terms which are determined from the data on low-energy elastic e-CO_2 scattering and vibrational excitation [22] and from ab initio potential energy surface for CO_2^- [23]. In a good approximation, f is independent of the cluster size N. However, more detailed studies [13], using a pseudopotential approach, show that $\mathrm{Re}f_0$ varies slowly between 0.387 and 0.372 a.u. when N changes from 3 to 22.

All terms in the expansion of $f(s,\rho)$ were assumed to be real except the zero-order term f_0. The parameter $\mathrm{Im}f_0$ responsible for IVR is the only free parameter in our calculations

Using these expansions, the logarithmic derivative f can be represented in matrix form and matched with the solution of vibrational close coupling equations in the region $r > r_0$. For CO_2, the basis for vibrational close coupling expansion should be constructed with the account of the Fermi resonances. For example, interaction between the levels ($\nu_1 = 1$, $\nu_2 = 0$) and ($\nu_1 = 0$, $\nu_2 = 2$) form the even Fermi dyad. Here the vibrational quantum number ν_1 is used for the symmetric stretch mode and ν_2 for the double-degenerate bending mode. Higher Fermi polyads (triads, tetrads and pentads) were also included in our calculations by representing the actual eigenstates of the vibrational Hamiltonian by linear combinations of symmetric stretch and bending vibrations [24,25]. For SF_6 the vibrational basis was supplemented by the vibrational functions of the infrared-active ν_3 mode because of the very large transition dipole moment for these vibrations.

The radial matrix of the outside solutions can be written as

$$\psi = \psi^- - \psi^+ S$$

where $\psi^\pm$ are matrices of the outgoing and ingoing solutions and S is the scattering matrix. The matching equation is solved for S from which we obtain elastic, vibrational excitation and attachment cross-sections.

3 Results and discussion

3.1 SF_6

In Figure 1 we present total, elastic and attachment cross-sections for e-SF_6 scattering for energies up to 0.22 eV. Strictly speaking, ERT fails at higher energies since we observe a violation of conservation of probability in this region. However, this violation is weak, and we therefore assume that elastic scattering and vibrational excitation calculations can be extended to higher energies (up to 0.4 eV) [7] using the same ERT parameters.

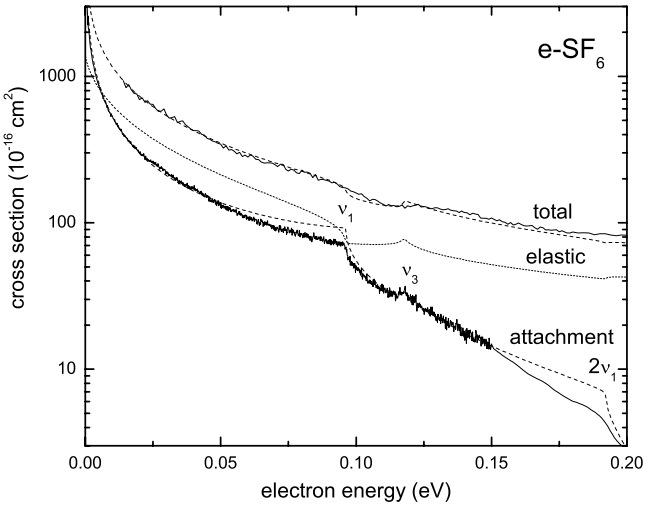

Fig. 1. Cross-sections for electron scattering by SF_6 molecules. Solid lines: experimental total and attachment cross-sections, dashed and dotted lines: theoretical cross-sections. Vibrational excitation thresholds are indicated by ν_1, ν_3 and $2\nu_1$.

For comparison we present experimental data for total scattering [21] and attachment [19,20] cross-sections to which the ERT parameters were fitted. We observe small deviations from the attachment experiment right below ν_1 and $2\nu_1$ thresholds. Otherwise the fit is very good: not only we reproduce the overall energy dependence and the absolute value of the cross-section, but also the cusp structures at ν_2 and ν_3 thresholds.

In dissociative attachment studies one of important and interesting questions is how the cross-section depends on the initial vibrational state of the molecule ν_i. This dependence determines the gas-temperature dependence of the cross-section [26]. The vibrational-state dependence is strong if the resonance anion potential energy curve crosses the neutral molecule curve at the internuclear distance outside the Franck-Condon region. In this case the capture cross-section, which contains the Franck-Condon factor, is strongly dependent on ν_i. For example in the CH_3X sequence (X = Cl, Br, I), the crossing occurs closer to the equilibrium internuclear separation as we proceed from Cl to I. Accordingly, the gas-temperature dependence of the cross-section is very strong in CH_3Cl but almost negligible in CH_3I [27]. The case of nondissociative attachment to SF_6 is different. There is no resonance state involved and the capture occurs into the virtual state of SF_6^- which then gets stabilized by IVR. Therefore, as can be seen from the formalism described above, there is no Franck-Condon factor involved, and the cross-section is not expected to be dependent on ν_i. Indeed, measurements at low energies [28–31] did not indicate any significant temperature dependence of attachment in e-SF_6 collisions.

However, our calculations show that the situation is somewhat more complicated. In Figure 2 we present attachment from different ν_{1i} states. We observe a clear dependence on initial ν_1, whereas no noticeable dependence on initial ν_{3i} was obtained. We should add, however,

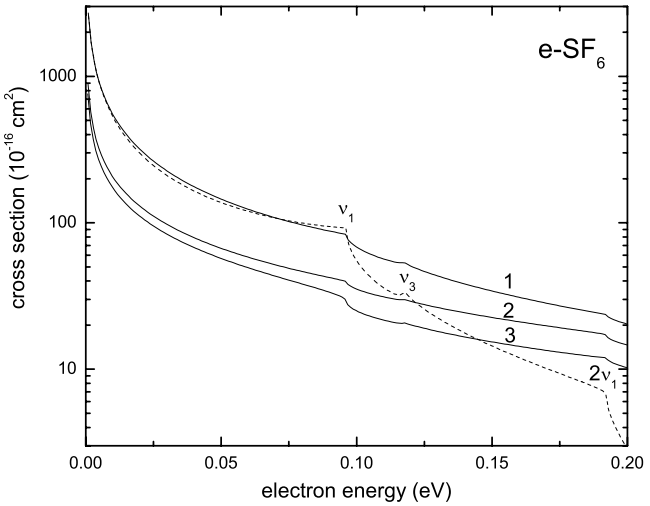

Fig. 2. Cross-sections for electron attachment from vibrationally excited SF_6 molecules. Numbers near the solid curves indicate the initial vibrational quantum number ν_1. Attachment from the ground state is given by the dashed curve with symbols ν_1, ν_3, $2\nu_1$ indicating vibrational excitation thresholds.

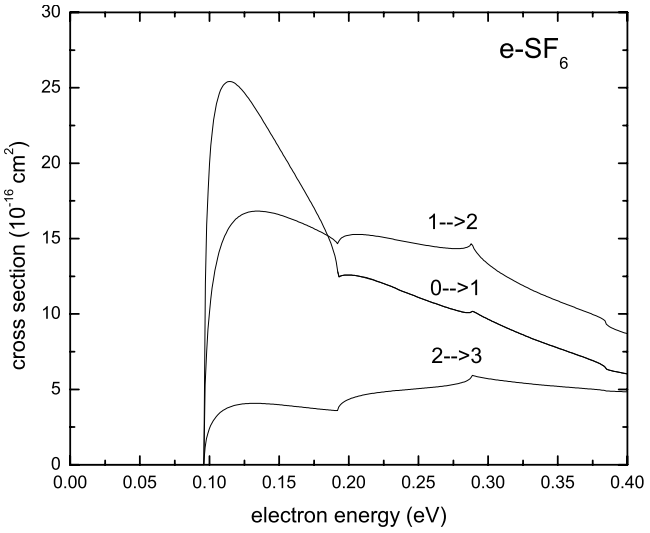

Fig. 3. Vibrational excitation of the symmetric ν_1 mode from the ground and vibrationally excited states.

that the ν_{1i} dependence is not strong enough to appear in the gas-temperature dependence of the cross-section for temperatures up to 1000 K. The explanation of the observed ν_{1i} dependence is based on the role of the virtual state. The anion energy as a function of the symmetric stretch coordinate crosses the neutral curve very close to the equilibrium internuclear separation for the neutral. Therefore for a vibrational state, whose probability density distribution is close to the equilibrium, the effect of the virtual state is strong. As a result, we observe a strong virtual-state effect for the ground state, and it becomes progressively weaker for excited state. This is also seen in the cusp structure at the $\nu_1 = \nu_{1i} + 1$ thresholds:

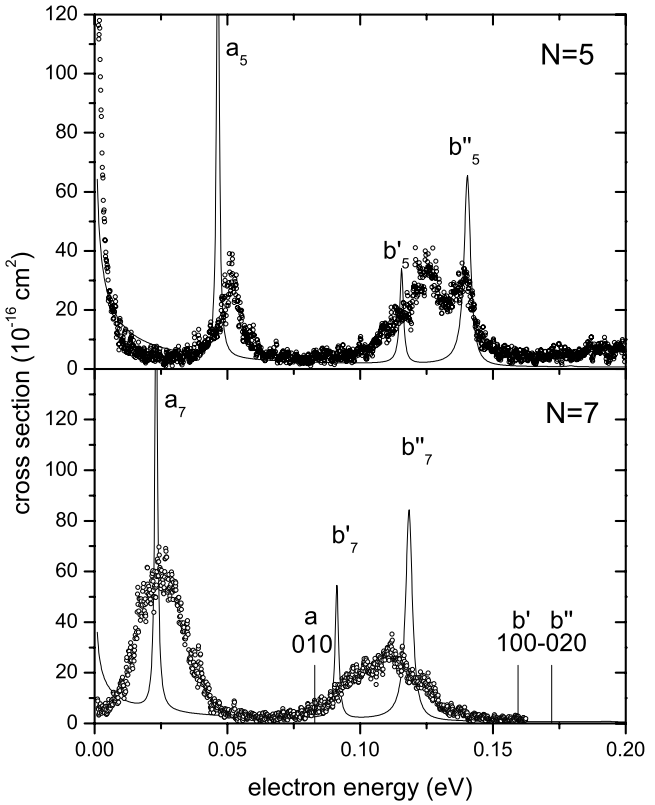

Fig. 4. Cross-section for electron attachment to $(CO)_N$ clusters, $N = 5$ and 7. Circles: experimentally observed yield of $(CO_2)_q^-$ ions, $q = 5$ and 7, normalized arbitrarily. Vibrational thresholds for neutral clusters of size N are labelled by vertical bars and letters a, b' and b'', whereas the position of corresponding VFRs are labelled by a_N, b'_N and b''_N.

for $\nu_{1i} = 0$ the cusp is very pronounced, but it becomes weaker for higher ν_{1i}.

The same effect can be seen in the scattering cross-sections. In Figure 3 we present cross-sections for vibrational excitation from the ground and low excited vibrational states. The threshold peak is very pronounced for excitation from the $\nu_{1i} = 0$ state, in agreement with experimental observations [7,32], whereas for higher ν_{1i} it gradually disappears.

3.2 CO_2 clusters

Attachment cross-sections for some selected cluster sizes are presented in Figures 4 and 5. We compare them with the experimentally observed attachment spectra [33].

Experimental data are presented for the *observed* size q of the cluster anions which is not necessarily the same as the size of the precursor $N \geq q$ because of the possible evaporation effect [2]

$$(CO_2)_N + e^- \rightarrow (CO_2)_q^- + (N-q)CO_2. \qquad (9)$$

Note also that the relative intensities of experimental spectra are subject to the density of the respective neutral

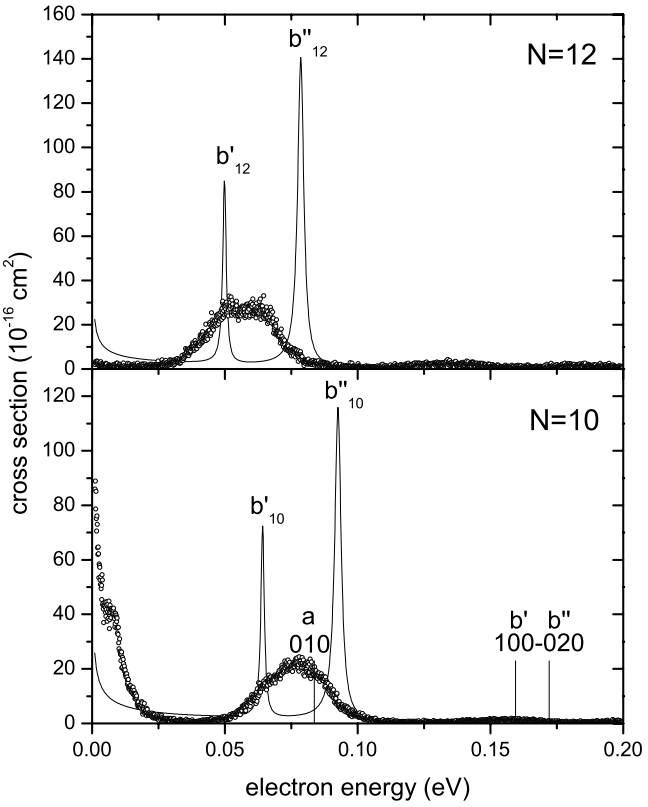

Fig. 5. The same as in Figure 4 for $N = 10$ and 12.

precursor clusters, thus they do not directly reflect relative cross-sections when one compares different precursor sizes. Therefore, for each N the experimental data are normalized arbitrarily.

Calculations were performed with a rather arbitrary choice of the parameter $\mathrm{Im}f_0 = -0.001$ a.u. which characterizes the coupling between the symmetric stretch mode in CO_2 and the bath modes in the cluster. The VFRs observed in attachment cross-sections are very narrow and confirm the major experimental findings. In particular, the most pronounced resonances are associated with the (010) and (100)–(020) thresholds corresponding to excitation of the Fermi monad and the even Fermi dyad respectively. All resonances are red-shifted relative to corresponding thresholds reflecting the positions of binding energies of electron in the field of the whole cluster [10,11]. The calculated splitting between different VFR dyad components is somewhat higher than the splitting between dyad components for the neutral molecule, since the presence of an extra electron creates an additional interaction leading to a repulsion between vibrational levels. This effect is in variance with observations: at $q = 5$ the experimentally observed distance between peaks is close to the separation between the two neutral dyad components, and only one peak is observed at higher q.

In this connection it is important to note that the theoretical peaks exhibit some selectivity in attachment to different components of the Fermi dyad, although this selectivity is much less pronounced than in vibrational excitation of monomers: the peak value of the lower resonance below the (100)–(020) threshold is about 2.0–1.5 times lower than that for the higher resonance whereas in vibrational excitation of monomers the two near-threshold peaks differ by two orders of magnitude [34,35]. In the attachment experiment the double-peak structure is observed only at $N = 5$, and both peaks are almost equal in magnitude. For higher N the double-peak structure disappears.

The difference can be explained by the broadening of the resonance peaks due to several reasons. First, for any particular $(CO_2)_q^-$ cluster ion, the width of the observed resonances is broadened by contribution of all involved neutral precursors of size $N \geq q$ which participate in VFR formation. For $q = 5$ the experimentally observed resonances exhibit the smallest widths, and it is likely that the attachment spectrum is predominantly associated with a single neutral precursor size. Some inhomogeneous broadening is still possible due to contribution of different conformations for this cluster size and due to the electron density fluctuations within the cluster. In particular, the fact that VFR is associated with excitation of *one* molecular unit, leads to the dependence of the resonance energy on the position of this unit within the cluster and contributes to further broadening [13]. Finally, some broadening effects could be possible due to the presence of excited molecular units within the clusters. As we discussed in the previous section, attachment to vibrationally excited SF_6 can be dependent on the vibrational quantum number. To investigate this effect in CO_2 clusters, we have calculated attachment from the first three excited vibrational state of CO_2, (010) monad and (100)–(020) dyad, in the cluster of size $N = 6$. In Figure 6 we present these cross-sections and compare them with attachment from the ground state. Very substantial changes in the positions and widths of VFRs is seen. In interpreting these results we have to take into account the strong anharmonicity effects in CO_2 due to the Fermi resonances: the positions of excited vibrational states in CO_2 are strongly nonequidistant.

In particular the first VFRs in attachment from the ground state are due to the (010) threshold (0.083 eV) and the threshold for excitation of the lower component of the (100)–(020) dyad (0.159 eV). At the same time the resonances in attachment from the (010) state (upper panel in Fig. 6) are due to the (100)–(020) dyad thresholds (0.077 and 0.089 eV relative to the (010) state). The triple-peak structure in attachment from the dyad states (lower panel in Fig. 6) is due to the triad thresholds. Because of this complicated threshold structure, we identify the resonances only for attachment from the ground state, as in Figures 4 and 5. As usual, the VFR positions are red-shifted relative to the corresponding thresholds, but these shifts are nonuniform due to the interaction between the resonances.

In summary, the anharmonicity effect leads to a strong dependence of the peak position on the initial vibrational state.

In addition to the strong anharmonicity effect we observe a substantial growth of the resonance width with the

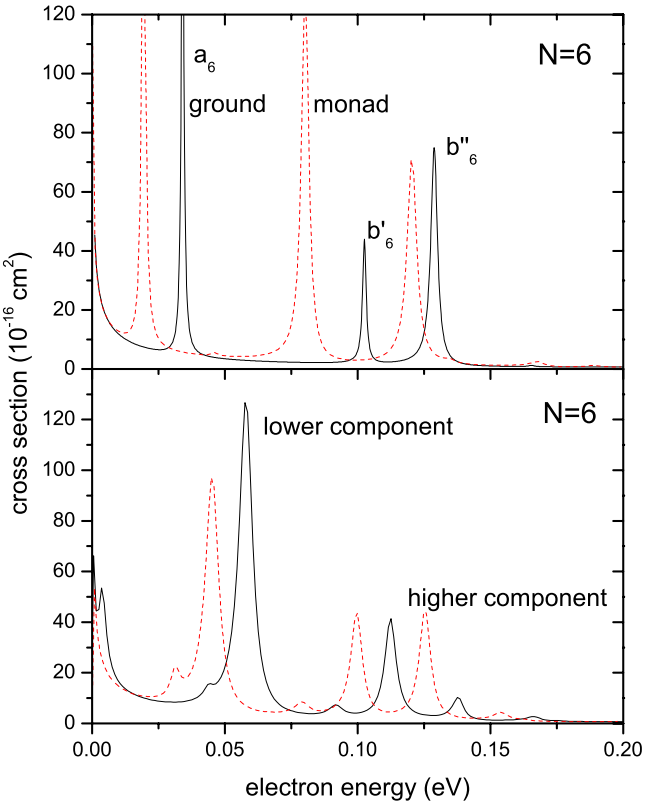

Fig. 6. Upper panel: attachment to the ground and the first excited (monad) state of the $(CO_2)_6$ cluster. Lower panel: attachment to the second and the third excited states (even dyad components). VFRs are identified only for attachment to the ground state using the same notation as in Figures 4 and 5.

initial vibrational quantum numbers. In our calculations the probability of capture in the negative-ion state is determined by the vibrational coupling. Since the coupling grows with the degree of excitation, so does the autodetachment width. The obtained strong dependence of the attachment cross-section on the initial vibrational state might provide an additional mechanism for resonance broadening observed in the experiment.

4 Conclusion

The simple generalization of the ERT approach employed in the present paper allowed us to describe a broad variety of phenomena observed in electron collisions with SF_6 molecules and CO_2 clusters: elastic scattering, attachment and vibrational excitation. We can also investigate how cross-sections for these processes depend on the initial vibrational quantum numbers of the target. This is an important supplement to experimental data because of the difficulty of obtaining data for selectively excited targets.

The author is thankful to H. Hotop and M. Allan for the fruitful collaboration. This work has been supported by the US National Science Foundation, Grant No. PHY-0354688.

References

1. T.F. O'Malley, Phys. Rev. **150**, 14 (1966)
2. H. Hotop, M.-W. Ruf, M. Allan, I.I. Fabrikant, Adv. At. Mol. Phys. **49**, 85 (2003)
3. M.A. Huels, I. Hahndorf, E. Illenberger, L. Sanche, J. Chem. Phys. **108**, 1309 (1998)
4. J.P. Gauyacq, A. Herzenberg, J. Phys. B **17**, 1155 (1984)
5. T. Uzer, Phys. Rep. **199**, 73 (1991)
6. M. Thoss, W. Domcke, J. Chem. Phys. **109**, 6577 (1998)
7. I.I. Fabrikant, H. Hotop, M. Allan, Phys. Rev. A **71**, 022712 (2005)
8. I.I. Fabrikant, H. Hotop, Phys. Rev. Lett. **94**, 063201 (2005)
9. J.M. Weber, E. Leber, M.-W. Ruf, H. Hotop, Phys. Rev. Lett. **82**, 516 (1999)
10. E. Leber, S. Barsotti, I.I. Fabrikant, J.M. Weber, M.-W. Ruf, H. Hotop, Eur. Phys. J. D **12**, 125 (2000)
11. E. Leber, S. Barsotti, J. Bömmels, J.M. Weber, I.I. Fabrikant, M.-W. Ruf, H. Hotop, Chem. Phys. Lett. **325**, 345 (2000)
12. P. Stampfli, Phys. Rep. **255**, 1 (1995)
13. I.I. Fabrikant, J. Phys. B **38**, 1745 (2005)
14. B.I. Schneider, M. LeDourneuf, P.G. Burke, J. Phys. B **12**, L365 (1979)
15. I.I. Fabrikant, Comm. At. Mol. Phys. **24**, 37 (1990)
16. I.I. Fabrikant, Phys. Rev. A **43**, 3478 (1991)
17. E.S. Chang, U. Fano, Phys. Rev. A **6**, 173 (1972)
18. J.P. Gauyacq, J. Phys. B **23**, 3041 (1990)
19. D. Klar, M.-W. Ruf, H. Hotop, Chem. Phys. Lett. **189**, 448 (1992)
20. H. Hotop, D. Klar, J. Kreil, M.-W. Ruf, A. Schramm, J.M. Weber, in: *The Physics of Electronic and Atomic Collisions*, edited by L.J. Dube, J.B.A. Mitchell, J.W. McConkey, C.E. Brion, AIP Conf. Proc. (AIP Press, Woodbury, N.Y., 1995), Vol. 360, p. 267
21. D. Field, N.C. Jones, J.P. Ziesel, Phys. Rev. A **69**, 052716 (2004)
22. S. Mazevet, M.A. Morrison, L.A. Morgan, R.K. Nesbet, Phys. Rev. A **64**, 040701 (2001)
23. T. Sommerfeld, J. Phys. B **36**, L127 (2003)
24. D.M. Dennison, Phys. Rev. **41**, 304 (1932)
25. D.M. Dennison, Rev. Mod. Phys. **12**, 175 (1940)
26. T.F. O'Malley, Phys. Rev. **155**, 59 (1967)
27. R.S. Wilde, G.A. Gallup, I.I. Fabrikant, J. Phys. B **33**, 5479 (2000)
28. D. Spence, G.J. Schulz, J. Chem. Phys. **58**, 1800 (1973)
29. Z. Lj. Petrović, R.W. Crompton, J. Phys. B **17**, 2777 (1985)
30. L.G. Christophorou, J.K. Olthoff, Adv. At. Mol. Phys. **44**, 155 (2000)
31. A. Rosa, F. Brüning, S.V.K. Kumar, E. Illenberger, Chem. Phys. Lett. **391**, 361 (2004)
32. K. Rohr, J. Phys. B **10**, 1175 (1977)
33. S. Barsotti, E. Leber, M.-W. Ruf, H. Hotop, Int. J. Mass Spectrom. **220**, 313 (2002)
34. M. Allan, Phys. Rev. Lett. **87**, 033201 (2001)
35. W. Vanroose, Z. Zhang, C.W. McCurdy, T.N. Rescigno, Phys. Rev. Lett. **92**, 053201 (2004)